Monte Carlo simulation of a cluster system with strong interaction and random anisotropy

L. Wang,[1] J. Ding,[2] H. Z. Kong,[2] Y. Li,[2] and Y. P. Feng[1]
[1]*Department of Physics, National University of Singapore, Lower Kent Ridge Road, Singapore 119260, Singapore*
[2]*Department of Material Science, National University of Singapore, Lower Kent Ridge Road, Singapore 119260, Singapore*
(Received 17 April 2001; published 7 November 2001)

The Monte Carlo method is used to study magnetic properties of amorphous rare-earth (RE) and transition-metal alloys, based on a model in which the magnetic units are magnetic clusters. Each cluster is assumed to possess a certain magnetic moment, which decreases with increasing temperature, and a Curie temperature T_c^{cluster}. A random distribution is assumed for the magnetic easy directions of the clusters. Monte Carlo simulations were carried out to simulate magnetization curves after zero-field cooling and magnetic hysteresis loops at different temperatures. The simulation results showed presence of two other critical temperatures T_{block} and T_c^{system} below T_c^{cluster}. Here T_{block} is the blocking temperature due to the anisotropy energy of clusters, while T_c^{system} is the freezing temperature due to interactions between clusters. If T_c^{system} is lower than T_{block}, the system behaves as a normal superparamagnetic material, characterized by a relatively weak effect of cluster correlation and/or dipole interaction. If T_c^{system} is higher than T_{block}, as in the case of many amorphous rare-earth and transition-metal alloys, it is possible to have three magnetic states, depending on the temperature: ferromagnetism when $T<T_c^{\text{system}}$, superparamagnetism with correlation when $T_c^{\text{system}}<T<T_c^{\text{cluster}}$, and paramagnetism when $T>T_c^{\text{cluster}}$. The freezing due to cluster interactions is characterized by a significant increase of remanence, while high coercivity is obtained below T_{block}. The simulation results were compared with the experimental measurements. The magnetic behaviors of amorphous rare-earth and transition-metal alloys are well described by the model.

DOI: 10.1103/PhysRevB.64.214410 PACS number(s): 75.50.Kj, 75.30.Gw, 75.60.Ej

I. INTRODUCTION

Amorphous rare-earth (RE) and transition-metal alloys have been insensitively studied[1–3] due to their interesting physical properties and potential applications. For example, their hard magnetic properties are promising for magnetic and magneto-optic recording. Despite these studies, however, the mechanisms for the observed magnetization and coercivity are not well understood. In earlier works,[4–6] we studied amorphous RE-Fe-based alloys, such as Nd-Fe-Al, Y-Fe-Al, Sm-Fe-Al, Gd-Fe-Al, and Dy-Fe-Al and observed the presence of inhomogeneity and formation of magnetic clusters in these materials. The behaviors of magnetization curves taken at different temperatures could be well explained using superferromagnetic theory, confirming the presence of clusters and strong interactions between them. Similar results have also been reported by others.[7,8] Inhomogeneity and clusters of 1–2 nm in size in these amorphous alloys can be clearly seen by transmission electron microscope.[9]

The most common approach for studying amorphous hard magnetic materials is the random magnetic anisotropy model proposed by Harris *et al.*[10] In this model, the magnetic property of an amorphous hard magnetic material is determined by two factors, the interaction between spins and the anisotropy energy of spins for randomly distributed easy directions. This model was very successful in describing the magnetic behaviors of many amorphous hard magnetic materials.[11–14] The random anisotropy model, however, was based on uniform amorphous structures and may not be applicable to inhomogeneous amorphous materials. Based on our experimental works,[4–6] we suggested that the anisotropy energy of the clusters and the interaction between the clusters are important factors affecting the properties of an inhomogeneous amorphous magnetic material.[4] Similar concepts have been used in the study of nanomagnets[15–21] where the magnetic features are determined by interaction between nanoparticles and anisotropy of individual nanoparticles. A calculation based on an analytic mean-field theory showed that the effect of cluster interactions can result in freezing into a ferromagnetic state for amorphous RE-Fe based alloys.[4,6] The simple mean-field analysis, however, cannot predict many other important magnetic features, such as coercivity and magnetic hysteresis.

In order to further explore the applicability of our cluster interaction model and to further investigate the mechanisms underlining the observed magnetic properties of inhomogeneous amorphous magnetic materials, we performed Monte Carlo simulations and calculated the magnetic hysteresis loops and zero-field-cooled (ZFC) magnetization curves of a magnetic cluster system. The Monte Carlo simulation enables the evaluation of many important magnetic parameters, such as blocking temperature (T_{block}) due to anisotropy, freezing temperature (T_c^{system}) due to cluster interactions, remanence, and coercivity in dependence on the cluster interaction energy and magnetic anisotropy energy. The simulation results have been compared with the experimental results of different amorphous rare-earth and transition-metal alloys. Excellent agreement is obtained between the experimental data and our simulation results.

II. HAMILTONIAN OF THE MAGNETIC CLUSTER SYSTEM

The Monte Carlo simulation was carried out using a system of 1000 clusters. The basic unit in the simulation is a cluster, and for each cluster, six nearest neighbors are con-

sidered when calculating the interaction between clusters. All the clusters possess a magnetic moment m and a uniaxial magnetic anisotropy energy $E_D = Dm^2$, where D is the magnetic anisotropy parameter of the cluster. A random distribution was assumed for the easy magnetization directions.

The Hamiltonian E of the cluster system is given as

$$E = -D\sum_i [\vec{n}_i \cdot \vec{m}_i(T)]^2 - \frac{1}{2}\sum_{i\neq j} J_{ij}\vec{m}_i(T)\cdot\vec{m}_j(T) - \vec{H}\sum_i \vec{m}_i(T), \quad (1)$$

where $m_i(T)$ is the magnetic moment of the ith cluster, $\vec{n}_i$ is a unit vector in the direction of the easy magnetization of the cluster, J_{ij} is the exchange interaction between the ith cluster and the jth cluster which is one of the nearest neighbors of cluster i, and $\vec{H}$ is the applied magnetic field.

The temperature dependence of the magnetic moment of a cluster is given by

$$m(T) = m_s f(T/T_c^{\text{cluster}}), \quad (2)$$

where m_s is the saturation magnetic moment of the cluster at zero temperature and T_c^{cluster} is the Curie temperature of the magnetic cluster. $f(T/T_c^{\text{cluster}})$ varies from 1 at zero temperature to zero at the Curie temperature. Assuming the cluster behaves as a bulk material, the function $f(T/T_c^{\text{cluster}})$ can be obtained from the Brillouin function with $\mu_{\text{spin}} = 2\mu_B$.[4,6] It is noted, however, that the cluster magnetization may decrease faster with temperature than bulk materials. At low temperature, it is given by an effective power law $M \propto 1 - BT^{\alpha}$, with a size-dependent, but structure-independent, exponent, as described in Refs. 22–24.

The coordinate system used in our calculation and the definitions of the magnetization and easy magnetization directions of a given cluster are illustrated in Fig. 1. The z axis is chosen to be along $\vec{H}$. The magnetization direction and easy direction of the ith cluster are specified by (θ_i, φ_i) and (σ_i, γ_i), respectively. In terms of these variables, the energy of the ith cluster can be written as

$$E_i = -Dm_i^2(T)(\sin\theta_i \sin\sigma_i \cos(\varphi_i - \gamma_i) + \cos\theta_i \cos\gamma_i)^2 - 1/2 J_{ij} m_i(T) m_j(T)\sum_j (\sin\theta_i \sin\theta_j \cos(\varphi_i - \varphi_j) + \cos\theta_i \cos\theta_j) - Hm_i(T)\cos\theta_i. \quad (3)$$

III. MONTE CARLO SIMULATION

A. Monte Carlo technique in our simulation

The Monte Carlo (MC) simulation technique is an effective approach in studies of systems with many degrees of freedom. During such a simulation, random numbers are used to simulate statistical fluctuations in order to generate the correct thermodynamical probability of distributions.[25,26]

A typical MC simulation consists of two steps: thermalization and evolution. During thermalization, the system is led adiabatically to its thermodynamical equilibrium. After the system reaches its thermal equilibrium, its dynamics can be studied and properties of interest as well as influence of external parameters can be obtained.

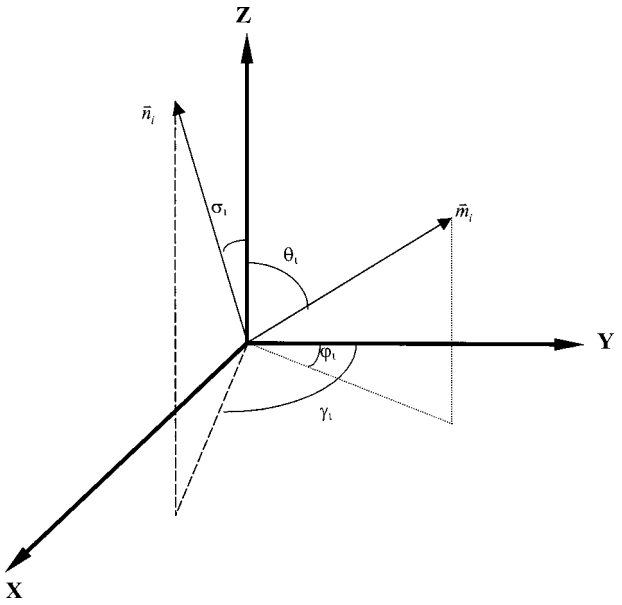

FIG. 1. The coordinate system and specifications of the magnetization and easy magnetization directions for a given cluster.

In this work, the standard Metropolis algorithm[25,26] with local dynamics[27–29] is used to simulate the ZFC magnetization curves (change of magnetization as a function of temperature under a constant field after zero-field cooling) and magnetic hysteresis loops (change in magnetization as a function of magnetic field under a constant temperature).

The simulations were performed with a set of 1000 clusters. The magnetic properties of each cluster are specified by four parameters: the direction of the easy axis is given by (σ_i, γ_i), while the magnetization direction is described by (θ_i, φ_i) (Fig. 1). The direction of the easy axis is kept fixed through out the simulation, and the values for σ_i and γ_i are chosen randomly in the ranges of $[0, \pi]$ and $[0, 2\pi]$, respectively. On the other hand, the direction of magnetization of the cluster is adjusted in each step and a small deviation, in the range of $(\delta\theta_i, \delta\varphi_i)$, from the direction in the previous step (θ_i, φ_i) is allowed. $\delta\varphi_i = 2\delta\theta_i$ was assumed in our calculation, since the range of φ_i,$(0,2\pi)$, is twice of that of θ_i,$(0,\pi)$. The energy difference ΔE between the new and current magnetization orientations is calculated from Eqs. (1) and (3). If $\Delta E \leqslant 0$, the magnetization is changed to the new state. Otherwise, the magnetization is allowed to change to the new orientation with a probability of $\exp(-\Delta E/k_B T)$ or to remain at its current orientation with a probability of $1 - \exp(-\Delta E/k_B T)$. Simulation of local dynamics allows the detection of metastable states, which are responsible for the hysteresis. The local dynamics also allows control of the acceptance rate of MC simulations. The larger the range of $\delta\theta_i$, the lower the acceptance rate. A constant acceptance rate means a constant rate of motion in the phase space.[27] In order to compare the simulation results at different temperatures, a constant acceptance rate is necessary. It is set to 35–37% in our simulation.

To simulate a magnetic hysteresis loop, the system must be initially thermolized at a desired temperature (sufficiently higher than the Curie temperature T_c^{cluster}) under a sufficiently high magnetic field (higher than its anisotropy field). In this thermolization process, the nonlocal dynamics [$\delta\theta \in (0,\pi)$] is used in order to bring the system to equilibrium quickly. After the system reaches equilibrium, local dynamics is used to simulate the magnetic hysteresis loop. Here $\delta\theta$ is adjusted to obtain the acceptance rate of 35–37%, which is followed by 10 000 Monte Carlo steps to thermalize the system. Finally, another 10 000 Monte Carlo steps are performed to collect data.

The procedure to simulate a ZFC magnetization curve is similar to that for a magnetic hysteresis loop. The system is first brought to equilibrium at a sufficiently high temperature in zero magnetic field. It is then cooled down to a low temperature (5 K) in zero field. Finally magnetization is recorded as a function of temperature in the heating process under a small constant magnetic field. The local dynamics is used to achieve equilibrium at high temperature. Here 10 000 Monte Carlo steps are used to thermalize the system at low temperature, and another 10 000 Monte Carlo steps are performed to collect data.

B. Blocking temperature T_{block} for a cluster system without interaction

In order to determine the blocking temperature T_{block} of the system as a function of magnetic anisotropy energy $E_D = Dm^2$, we simulated ZFC magnetization curves (M/M_s) under a constant magnetic field of 500 Oe. The effect of cluster interaction is not considered in this case [J is set to 0 in Eq. (1) during the simulation].

The MC method is a good technique for calculating properties of magnetic materials at finite temperature.[25,26] However, its main drawback is that individual MC steps do not correspond to real time, but are sampling of its phase at a certain rate. The time scale is always a very important issue when nonequilibrium phenomena are simulated.[30,31] In a recent work,[31] Smirnov-Rueda *et al.* compared the Monte Carlo method with Langevin dynamics and provided new insights to the interpretation of the Monte Carlo process, leading to the implementation of a new algorithm where the Monte Carlo step is time quantified. According to the work of Smirnov-Rueda *et al.*, it is possible to choose the trial step for a MC step in such way that a MC step corresponds to a real-time interval. In the present work, the simulation results of ZFC curves were used to quantify the time scale (consisting of 10 000 Monte Carlo steps for thermalization and 10 000 Monte Carlo steps for data collection).[27]

The blocking temperature (T_{block}) due to anisotropy energy is given by the maximum of magnetization in a ZFC curve.[32–35] In a superparamagnetic system, the thermofluctuation can be described by a relaxation time τ, which is essentially the average time it takes to reverse the magnetization direction of a cluster, and is determined by the magnetic anisotropy energy of the cluster,

$$1/\tau = f_0 \exp\left(-\frac{Dm^2}{k_B T}\right), \tag{4}$$

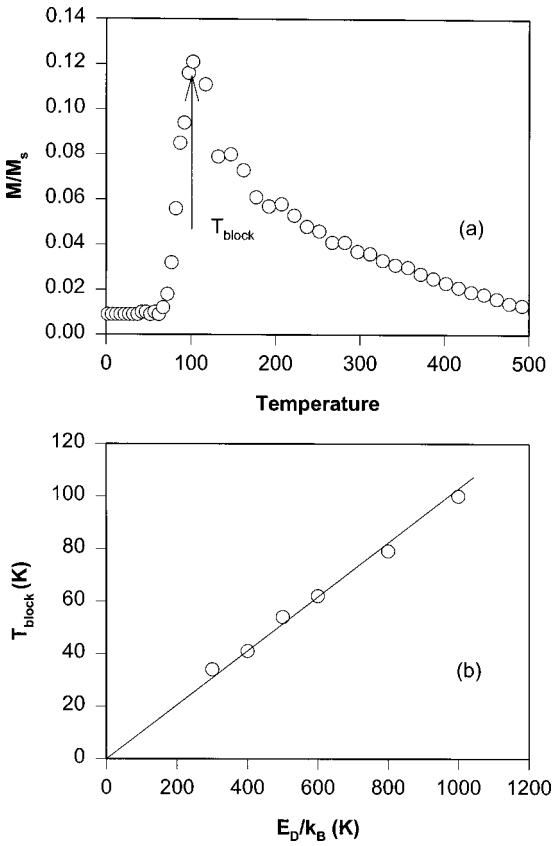

FIG. 2. (a) The simulated ZFC curve of the cluster system with $E_D/k_B = 1000$ K and $E_J/k_B = 0$ K. The blocking temperature is given by the maximum of the ZFC curve. (b) Dependence of blocking temperature T_{block} on the anisotropy energy E_D/k_B.

where Dm^2 is the anisotropy energy, T is the temperature, k_B is Boltzmann's constant, and f_0 is a constant (10^9 Hz).[36]

In our simulation, the MC acceptance rates are set to a narrow range of 35%–37%. Therefore, the rate of motion in phase space is almost constant. A ZFC curve for $E_D/k_B = 1000$ K obtained at a constant magnetic field of 500 Oe is shown in Fig. 2(a). A maximum near 100 K [or minimum of the reverse of magnetic susceptibility, as shown in Fig. 3(b)] is seen clearly in the ZFC curve, which gives the blocking temperature T_{block}.

The blocking temperature obtained from ZFC curves is shown in Fig. 2(b) as a function of E_D. From Eq. (4), T_{block} is expected to increase linearly with E_D/k_B when the relaxation time τ is a constant. The linear relationship between T_{block} and E_D/k_B shown in Fig. 2(b) indicates that the Monte Carlo simulation can reasonably describe the magnetic character of a cluster system. Furthermore, the slope of the straight line in Fig. 2 yields a value of approximately 10 for the ratio $Dm^2/k_B T_{\text{block}}$. Based on this and using Eq. (4), the relaxation time can be estimated to be in the order of 10^{-5} sec., which is about the same as the sampling time of a Mössbauer spectrometer, which is widely used for the estimation of blocking temperature for various superparamagnetic materials. Typical magnetic measurements are done over a time scale of 10 sec.[36] The increase of the Monte Carlo time scale from 10^{-5} to 10 sec can be achieved by

increasing the number of MC steps. However, a small increase in the Monte Carlo time scale can lead to a dramatic increase in the required number of Monte Carlo steps during a simulation. It is, therefore, unrealistic to increase the number of MC steps significantly because of limited computing resources. A short Monte Carlo time scale results in higher critical temperatures (e.g., T_{block}) than the values expected for a measurement time scale of 10 sec. For $E_D/k_B = 1000\,\text{K}$, the value of T_{block} estimated from our Monte Carlo simulation is 97 K, while the value calculated from Eq. (4) using the experimental time scale of 10 sec is 40 K. We can therefore conclude that our Monte Carlo simulation yields acceptable T_{block} values.

C. Simulation results and analysis

To increase the efficiency of the MC simulation, magnetic parameters such as Curie temperature T_c^{cluster}, magnetic moment of a cluster m_s, and magnetic anisotropy energy Dm^2 were allowed to vary only within predefined ranges which were chosen based on our previous measurements and analysis.[4,6] In our previous work, we successfully analyzed the magnetic behaviors of amorphous rare-earth and transition-metal alloys using a mean-field approach.[4] It was shown that the magnetic moment of a cluster is about $1000\mu_B$. Using the saturation magnetization of the well-known $Nd_2Fe_{14}B$ compound, $1000\mu_B$ corresponds to a particle size of 1.9 nm, which is in good agreement with the expected cluster size in these materials.[7] Clusters of approximately 1.2 nm were also reported by Klamer *et al.*[9] in such materials. Based on these, the magnetic moment of a cluster is fixed at $1000\mu_B$ in our simulation. The energy of interaction between clusters, E_J/k_B, was estimated to be in the range of 100–400 K using the mean-field analysis,[4] which was used in the MC simulation. The value of T_c^{cluster} was fixed at 550 K, since many magnetic measurements have shown that the Curie temperatures of many amorphous rare-earth and transition-metal alloys are in the range of 500–600 K.

The magnetic anisotropy energies of amorphous rare-earth and transition-metal alloys remain unknown. Assuming that the cluster has a similar structure of a rare earth containing crystalline structure, the magnetic anisotropy can possibly range from $E_D/k_B = 5440\,\text{K}$ for the hard magnetic $Nd_2Fe_{14}B$ phase to $E_D/k_B = 120\,\text{K}$ for the soft magnetic Fe_3B phase.

Figure 3(a) shows the ZFC magnetization curves of cluster systems with $E_D/k_B = 1000\,\text{K}$ and $E_J/k_B = 0$, 25, 200, and 300 K respectively. A constant applied magnetic field of 500 Oe was assumed in our calculation. The inverse of the magnetic susceptibility, $1/\chi$, was obtained by $H/(M/M_s)$ and the results are shown in Fig. 3(b) as a function of temperature. The maximum of magnetization (M/M_s) in Fig. 3(a) represents the blocking temperature T_{block} for $E_J = 0$ (noninteracting clusters). With the increase of the interaction energy E_J, the maximum of M/M_s shifted slightly to higher temperatures. In the $1/\chi$ vs. temperature curves in Fig 3(b), T_{block} is given by the minimum of $1/\chi$. Again, T_{block} does not change significantly with cluster interaction energy E_J. For

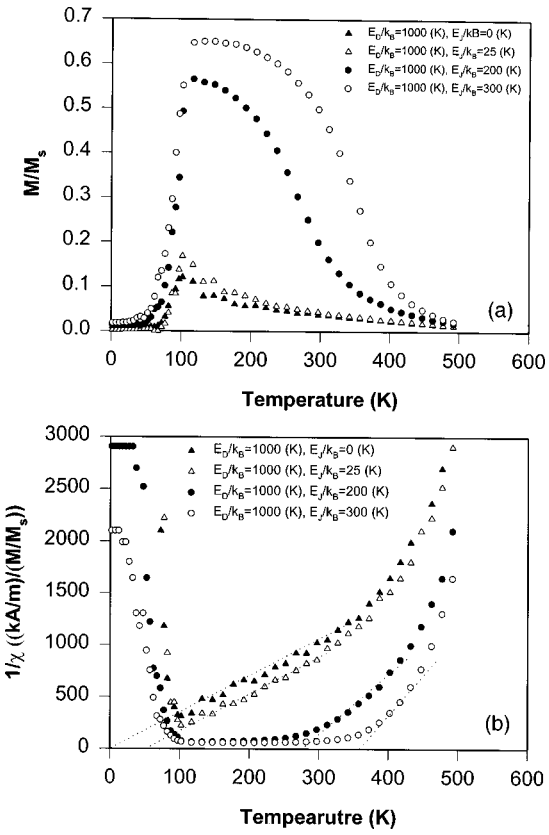

FIG. 3. The simulated ZFC (a) and inverse of susceptibility $1/\chi$ (b) curves for $E_D/k_B = 1000\,\text{K}$ and various values of E_J.

$E_D/k_B = 1000\,\text{K}$ and $E_J = 0$, the extrapolation of the linear part of the $1/\chi$ vs temperature curve at high temperature is expected to pass through the origin according to the theory of superparamagnetism.[36] $1/\chi$ remains small for a certain temperature range before increasing rapidly with temperature. The extrapolation of the quasilinear part of the $1/\chi$ curve intersects the temperature axis at a finite temperature value which shifts to higher temperature as interaction energy E_J increases. This temperature represents another critical temperature (T_c^{system}) which is the freezing temperature due to the interaction and will be discussed later.

Figure 4 shows the calculated ZFC and $1/\chi$ curves for a constant interaction energy ($E_D/k_B = 200\,\text{K}$), but different cluster anisotropy energies ($E_D/k_B = 200$, 1000, 2000, and 3000 K, respectively). The results show that T_c^{system}, given by the intersection of the extrapolation of the linear portion of the curve with the temperature axis in Fig. 4(b), remains almost the same for various anisotropy energies. The independence of T_c^{system} on anisotropy energy demonstrates that T_c^{system} is a result of the cluster interaction. On the other hand, the position of the minimum in $1/\chi$ shifts to higher temperature with increasing E_D. This confirms that the minimum represents the blocking temperature due to magnetic anisotropy. We can therefore conclude that there exist two critical temperatures in the cluster system, T_{block} and T_c^{system}. Here T_{block} is due to the anisotropy energy of clusters, while T_c^{system} is due to cluster interactions.

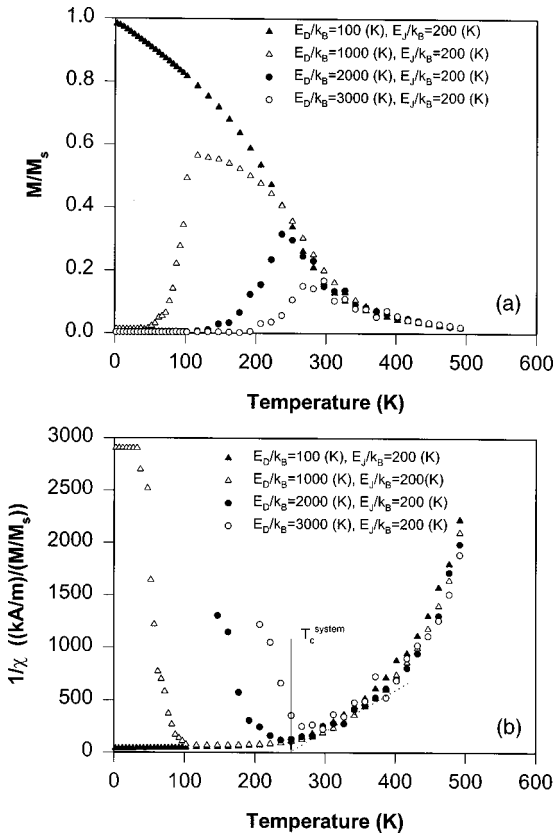

FIG. 4. The simulated ZFC (a) and inverse of susceptibility $1/\chi$ (b) curves for $E_J/k_B=200$ K and various values of E_D.

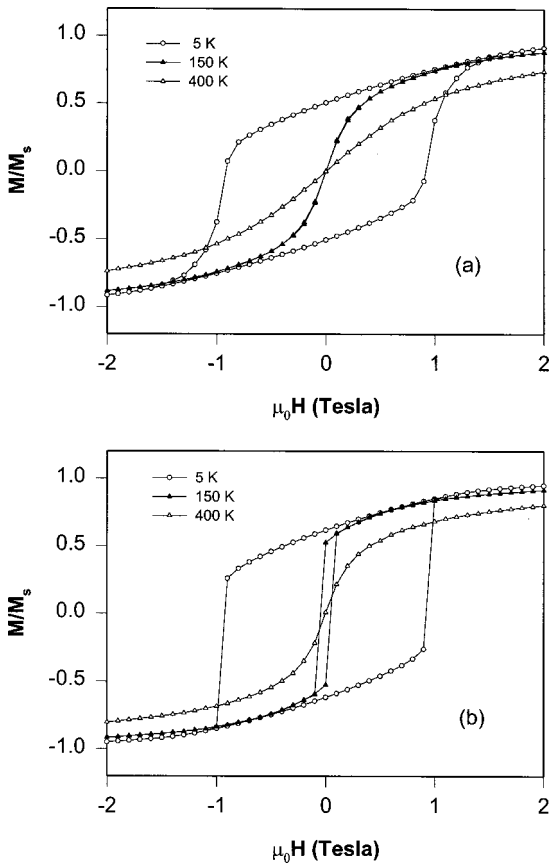

FIG. 5. The simulated magnetic loops at various temperatures for $E_D/k_B=1000$ K and $E_J/k_B=0$ (a) and 200 K (b), respectively.

Figure 5 shows the simulated hysteresis loops at various temperatures for two specimens, with $E_D/k_B=1000$ K and $E_J/k_B=0$ [Fig. 5(a)] and 200 K [Fig. 5(b)], respectively. Figure 6 shows the change of coercivity and remanence, respectively, with different temperatures for the same two systems. It is clear that the system with $E_J/k_B=0$ becomes superparamagnetic when the temperature is higher than T_{block}. Both coercivity and remanence are zero [Fig. 6(a)] above T_{block}, and the magnetization curves are typical of superparamagnetism [Fig. 5(a)]. Both the coercivity and remanence increase rapidly when T is reduced below T_{block}, as shown in Fig. 6(a). Such a feature is also found in a wide range of superparamagnetic systems.[4–6,36]

Similar results were obtained for nonzero but small interaction energy if T_c^{system} is below T_{block} (for example, for $E_J/k_B=25$ K shown in Fig. 3). This indicates that the ferromagnetic state is present when $T<T_{\text{block}}$, if T_c^{system} is below T_{block} and magnetic anisotropy plays the dominant role in this case.

For the system with $E_J/k_B=200$ K, T_c^{system} is well above T_{block} as shown in Figs. 2 and 3. A significant increase of remanence is observed when the temperature is below T_c^{system}. However, coercivity remains at a low level. High coercivity is found when the temperature is below T_{block} [Fig. 6(b)]. The hysteresis loop shown in Fig. 5(b) in the temperature range between T_{block} and T_c^{system} exhibits typical soft magnetic behavior. These indicate that the cluster interactions lead to a ferromagnetic state below T_c^{system}, while high coercivity requires the freezing below the blocking temperature. When $T_{\text{block}}<T<T_c^{\text{system}}$, the cluster interactions lead to a ferromagnetic coupling of the magnetic clusters. However, the thermal energy is high in comparison with the magnetic anisotropy energy. Therefore, the low coercivity values are due to easy flip or thermal excitation when $T>T_{\text{block}}$.

For amorphous rare-earth and transition-metal alloys, T_c^{system} is often higher than T_{block}.[4] Our Monte Carlo simulation results suggest the following magnetic behaviors for the cluster systems: paramagnetism when $T>T_c^{\text{cluster}}$, superparamagnetism with strong correlation when $T_c^{\text{system}}<T<T_c^{\text{cluster}}$, ferromagnetic with low coercivity when $T_{\text{block}}<T<T_c^{\text{system}}$, and ferromagnetic with higher coercivity when $T<T_{\text{block}}$, as schematically shown in Fig. 7.

Figure 8 shows the magnetic hysteresis loops at 5 K for a constant interaction energy of $E_J/k_B=300$ K and various values of magnetic anisotropy energy (E_D/k_B), ranging from 5540 K (corresponding to the hard magnetic phase $Nd_2Fe_{14}B$) to 120 K (corresponding to soft magnetic Fe_3B). From the simulated results, we can conclude that the coercivity is mainly determined by the magnetic anisotropy energy at such a low temperature. It is interesting to note that the hysteresis loop with $E_D/k_B=5540$ K describes the isotropic $Nd_2Fe_{14}B$ ($M_r=0.5M_s$ and $H_c=0.48H_{\text{an}}$ with $H_{\text{an}}=15$ T, as given by the Stoner-Wohlfarth model[9]) very well. With decreasing E_D, coercivity decreases, while remanence

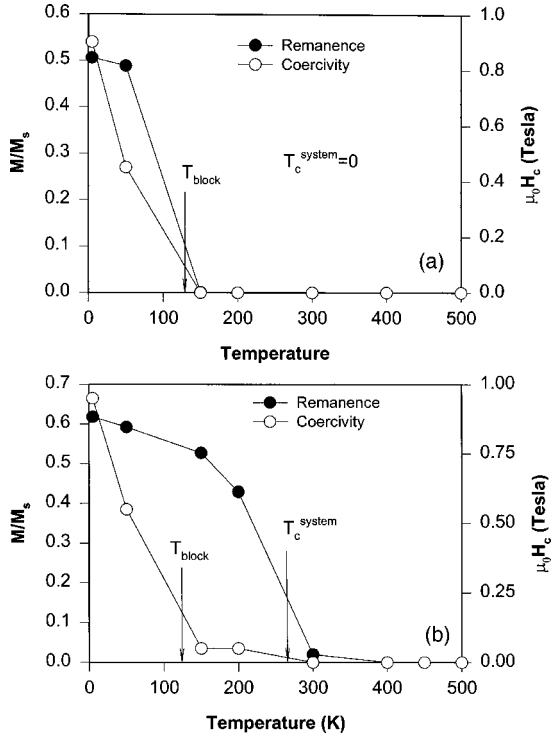

FIG. 6. The simulated temperature dependence of coercivity $\mu_0 H_c$ and relative remanence M_r/M_s for $E_D/k_B=1000\,\mathrm{K}$ and $E_J/k_B=0$ (a) and 200 K (b), respectively.

increases. For $E_D/k_B=120\,\mathrm{K}$, the hysteresis loop became highly square, indicating remanence enhancement resulting from cluster interactions. Remanence enhancement has been reported in nanocrystalline materials due to strong interactions between neighbored grains.[21,37]

IV. MAGNETIC MEASUREMENTS ON AMORPHOUS RE-Fe-BASED ALLOYS

We have also carried out direct measurements of magnetic properties of amorphous RE-Fe-based alloys. The alloys were prepared using melt-spinning technique. The experimental details were described elsewhere.[4–6] The experimental results were compared with the results obtained from our Monte Carlo simulations.

A. $Y_{60}Fe_{30}Al_{10}$

Yttrium has similar chemical properties as rare-earth elements. But Y is nonmagnetic. Ten percent of Al was used to enhance the formability of amorphous structure.[4–6,8] Figure 9 shows the magnetic hysteresis loops and magnetization curves of $Y_{60}Fe_{30}Al_{10}$ at various temperatures. It can be seen that all the magnetization curves exhibit typical character of superparamagnetism except the hysteresis loop obtained at 4.2 K. It was reported previously[4] that paramagnetism appears at temperature above 355 K, suggesting that $T_c^{\mathrm{cluster}}=355\,\mathrm{K}$. The ZFC and FC curves and temperature dependence of inverse susceptibility of $Y_{60}Fe_{30}Al_{10}$ are shown in Figs. 10 and 11, respectively. From the maximum of magnetization and minimum of inverse of susceptibility, $1/\chi$, T_{block} is estimated to be 13 K. Extrapolation of the quasilinear part of the $1/\chi$ curve [Fig. 12(a)] results in a T_c^{system} of approximately 5 K, which is below T_{block}. According to the mean-field analysis (Langevin function) given in Ref. 4, the cluster interaction energy in $Y_{60}Fe_{30}Al_{10}$ is much weaker than those in other RE-Fe-based alloys. Figure 12(a) shows that both the coercivity and remanence are zero when $T>T_{\mathrm{block}}$ and increase when the temperature is below the blocking temperature. This behavior is expected for a superparamagnetic system with weak interactions between particles.[4,36]

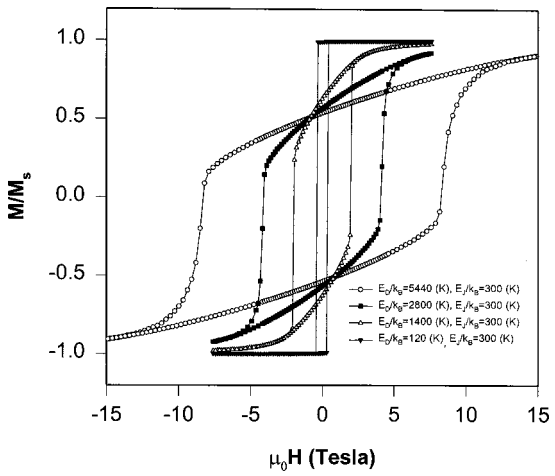

FIG. 8. The simulated magnetic loops at 5 K for $E_J/k_B=300\,\mathrm{K}$ and various values of E_D.

B. NdFeAl

Figure 13 shows the magnetization curves of NdFeAl measured at a wide range of temperature. From the magnetization curves, T_c^{cluster} is estimated to be around 300 K. Values for the two critical temperatures, $T_c^{\mathrm{system}}=125\,\mathrm{K}$ and

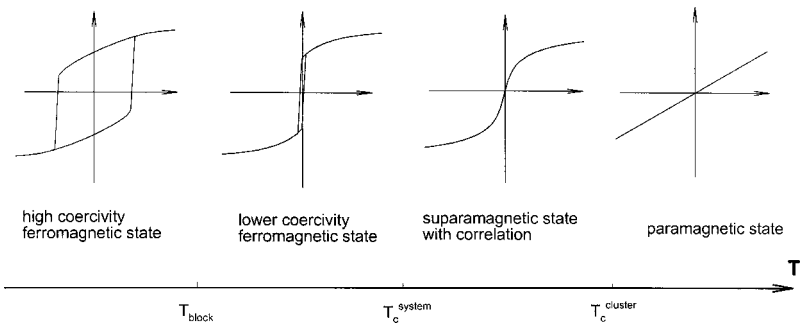

FIG. 7. The schematic illustration of magnetic loops of amorphous rare-earth and transition-metal alloys in different temperature regions.

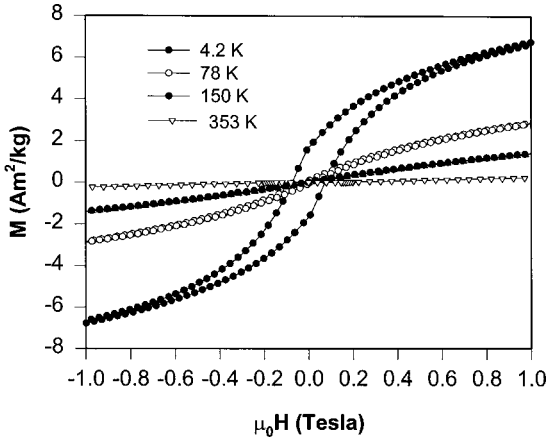

FIG. 9. The magnetic hysteresis loops of $Y_{60}Fe_{30}Al_{10}$ measured at various temperatures.

$T_{block}=75$ K, can be obtained from the ZFC and FC curves given in Fig. 10(b) and the $1/\chi$ curve given in Fig. 11(b). This indicates that the strong cluster interactions result in a ferromagnetic coupling between clusters with a critical temperature of 125 K. The temperature dependence of the coercivity and remanence are shown in Fig. 12(b). Remanence increases when temperature is reduced below 125 K, while coercivity starts to increase when temperature is reduced below $<T_{block}$. This behavior agrees well with prediction by our Monte Carlo simulation, as shown in Fig. 6(b).

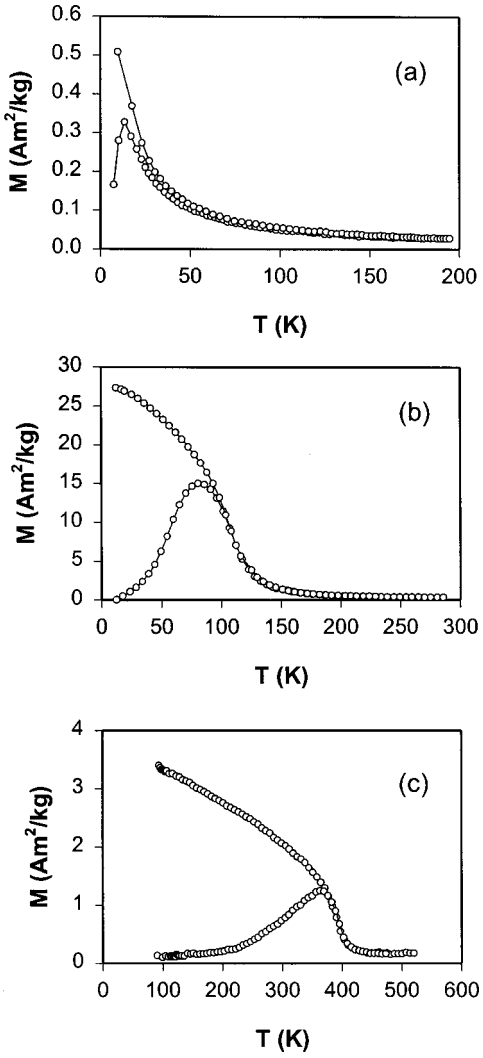

FIG. 10. The experimental ZFC and FC curves for (a) $Y_{60}Fe_{30}Al_{10}$, (b) NdFeAl, and (c) $Nd_{60}Fe_{30}Al_{10}$.

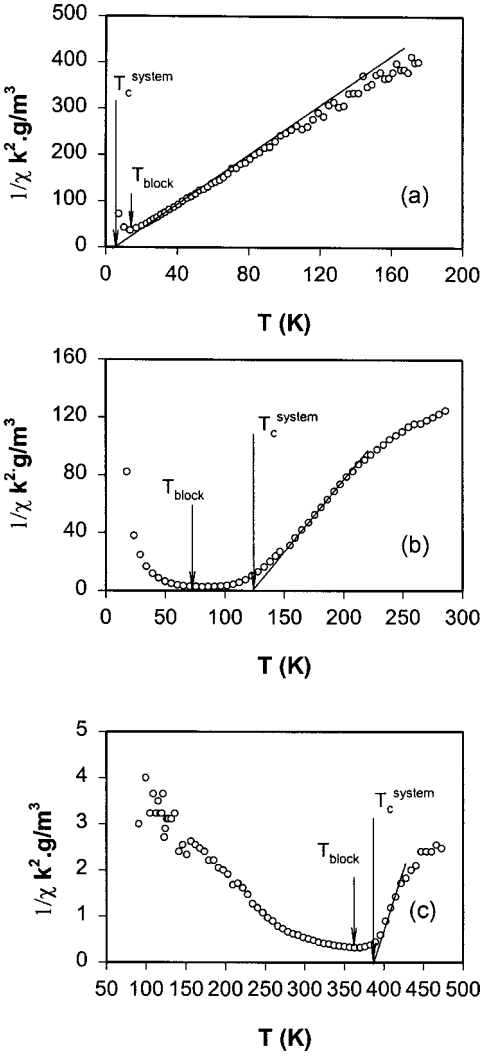

FIG. 11. The experimental $1/\chi$ vs temperature curves for (a) $Y_{60}Fe_{30}Al_{10}$, (b) NdFeAl, and (c) $Nd_{60}Fe_{30}Al_{10}$.

C. $Nd_{60}Fe_{30}Al_{10}$

An increase in Nd concentration compared to NdFeAl led to a shift of the critical temperatures to higher temperature. From our magnetic measurements, T_c^{cluster} for the $Nd_{60}Fe_{30}Al_{10}$ system was estimated to be 550 K. Here T_c^{system} and T_{block} are fairly close to each other, given by 380 and 360 K, respectively, as shown in Figs. 10(c) and 11(c). Comparison between $Y_{60}Fe_{30}Al_{10}$ and $Nd_{60}Fe_{30}Al_{10}$ shows that replacement of nonmagnetic Y by Nd enhances the Curie temperature T_c^{cluster}. The cluster interaction is strongly reinforced at the same time. It is certain that the high blocking temperature in $Nd_{60}Fe_{30}Al_{10}$ is associated with high magnetic anisotropy, due to the presence of Nd. It is well known

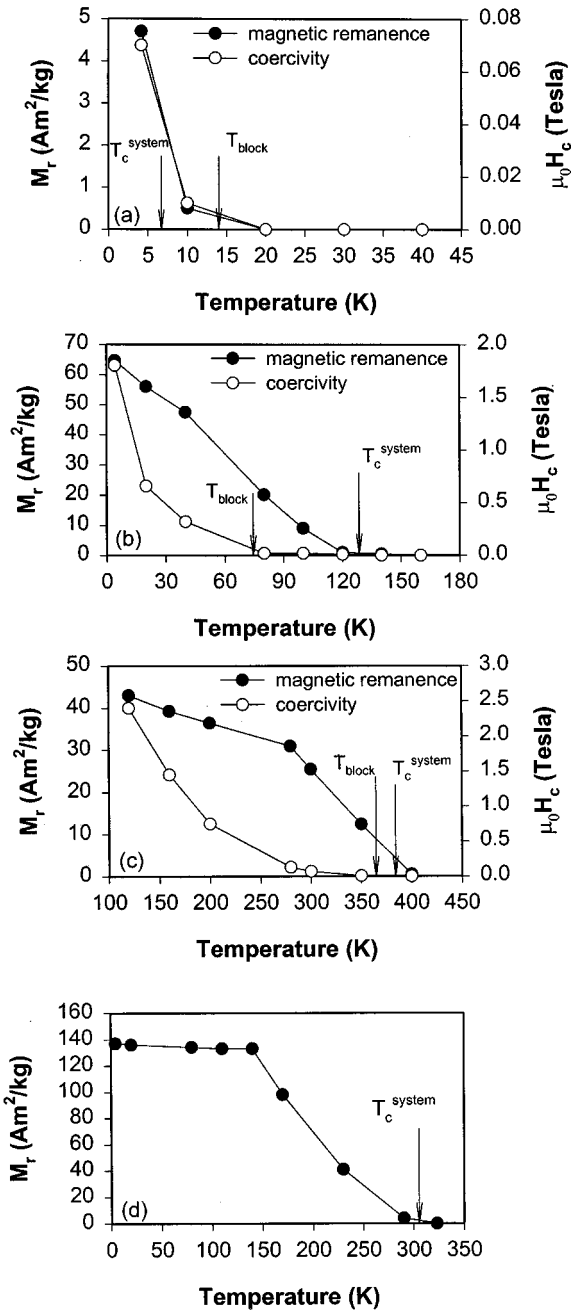

FIG. 12. The experimental temperature dependence of coercivity $\mu_0 H_c$ and remanence M_r for (a) $Y_{60}Fe_{30}Al_{10}$, (b) NdFeAl, (c) $Nd_{60}Fe_{30}Al_{10}$, and (d) remanence M_r for $Gd_{60}Fe_{30}Al_{10}$.

that compounds containing Nd often possess high magnetic anisotropy due to their high Steven's constant.[38] The higher blocking temperature of $Nd_{60}Fe_{30}Al_{10}$ compared to that of NdFeAl is probably due to the increase in magnetic anisotropy as a result of higher Nd concentration.

The remanence of $Nd_{60}Fe_{30}Al_{10}$ increases with decreasing temperature when $T<T_c^{system}$ [Fig. 12(c)], in agreement with results of our Monte Carlo simulation (Figs. 5 and 6). The coercivity H_c starts to increase when temperature is reduced below $T<350$ K, which is close to T_{block}.

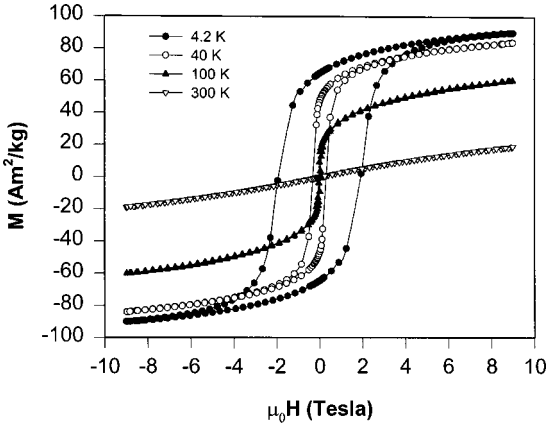

FIG. 13. The experimental magnetic loops of NdFeAl measured at various temperatures.

D. $Gd_{60}Fe_{30}Al_{10}$

The anisotropy energy of magnetic clusters in $Gd_{60}Fe_{30}Al_{10}$ is expected to be low since Gd is an *S*-state rare-earth ion. The values of $T_c^{cluster}$ and T_c^{system} obtained in our study are ~450 and ~300 K, respectively (Fig. 14), while T_{block} was measured to be lower than 5 K, which is much lower than that of $Nd_{60}Fe_{30}Al_{10}$, confirming the low magnetic anisotropy in $Gd_{60}Fe_{30}Al_{10}$.

When $T<T_c^{system}$, $Gd_{60}Fe_{30}Al_{10}$ is a soft magnetic material. Its coercivity is nearly zero in the temperature range

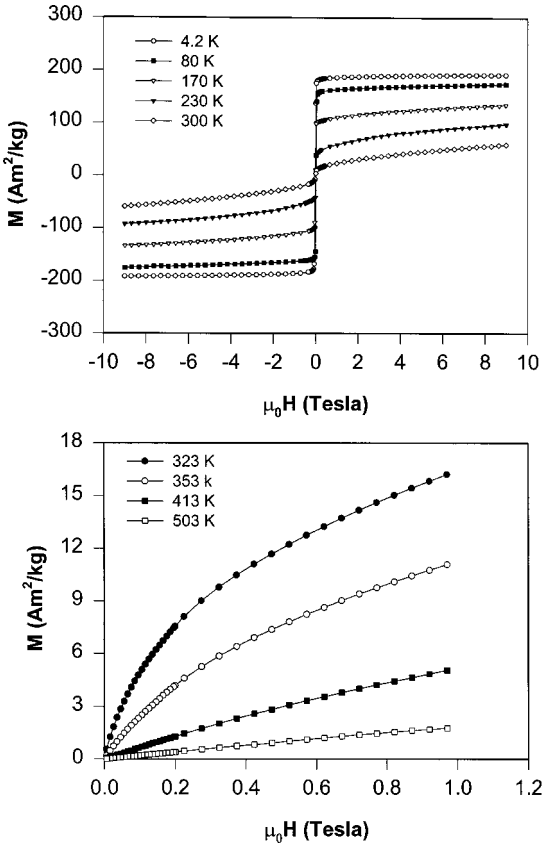

FIG. 14. The experimental magnetic loops of $Gd_{60}Fe_{30}Al_{10}$ measured at various temperatures.

from 4.2 to 300 K, as shown in Fig. 14. Its remanence is shown as a function of temperature in Fig. 12(d). The remanence increases with decreasing temperature when $T < T_c^{\text{system}}$ (~ 300 K), as predicted by our Monte Carlo simulation (Fig. 6). The observed magnetic properties of $Gd_{60}Fe_{30}Al_{10}$ fully agree with the results of a Monto Carlo simulation which predicts that the material with low magnetic anisotropy energy is soft magnetic.

In our previous studies,[4–6] high coercivity values were obtained in $R_{60}Fe_{30}Al_{10}$ with R being Nd, Pr, Sm, or Dy, whereas the RE element has a nonzero magnetic dipole moment. High coercivity values have been reported in many RE-(Fe, Co)-based amorphous materials,[1–8] including magnetic recording media.[39] It is believed that the high coercivity values in these materials are due to the large magnetic anisotropy of RE ions with nonzero dipole moment.

V. SUMMARY

Our previous magnetic and Mössbauer studies on amorphous rare-earth and transition-metal alloys suggested the formation of clusters. Inhomogeneity and clusters with a size of 1–2 nm were observed in these materials. In this work, we have proposed a model to describe the magnetic features of these cluster systems.

The magnetic units in this model are clusters. Each magnetic cluster is assumed to possess a magnetic moment of $1000\mu_B$ and a Curie temperature T_c^{cluster} of 550 K, which were obtained from previous magnetic studies. Assuming a random distribution for the easy magnetization directions of clusters, Monte Carlo simulations were carried out to simulate the magnetization curve after a zero-field cooling and magnetic hysteresis loops at various temperatures.

Two critical temperatures T_{block} and T_c^{system} below the Curie temperature were obtained, where T_{block} is the blocking temperature due to the cluster anisotropy energy and T_c^{system} is the freezing temperature due to the interaction between clusters. If T_c^{system} is higher than T_{block}, as for many amorphous rare-earth and transition-metal alloys, ferromagnetic coupling between clusters appears below T_c^{system}. However, hard magnetic properties are found below T_{block}. Our simulation results showed that the coercivity at low temperature is mainly determined by the anisotropy energy. The interaction between clusters has a little effect on the coercivity.

Magnetic measurements were performed on several amorphous rare-earth and transition-metal alloys. Typical superparamagnetic properties were observed for $Y_{60}Fe_{30}Al_{10}$ due to its low cluster interaction energy resulting from the nonmagnetic Y element. For NdFeAl and $Nd_{60}Fe_{30}Al_{10}$, T_c^{system} and T_{block} can be clearly defined in their ZFC curves. The temperature dependence of coercivity and remanence agrees well with results of the Monte Carlo simulation. Soft magnetic properties were evident in $Gd_{60}Fe_{30}Al_{10}$, which is a result of its low magnetic anisotropy energy due to the zero dipole moment of Gd.

[1] R. C. Talyor, T. R. McGuire, J. M. D. Coey, and A. Gangulee, J. Appl. Phys. **49**, 2885 (1978).
[2] J. J. Croat, Appl. Phys. Lett. **39**, 357 (1981).
[3] S. G. Cornelison, D. J. Sellmyer, J. G. Zhao, and Z. D. Chen, J. Appl. Phys. **53**, 2330 (1982).
[4] L. Wang, J. Ding, Y. Li, Y. P. Feng, X. Z. Wang, N. X. Phuc, and N. H. Dan, J. Appl. Phys. **89**, 8046 (2001).
[5] L. Wang, J. Ding, Y. Li, Y. P. Feng, X. Z. Wang, N. X. Phuc, and N. H. Dan, J. Magn. Magn. Mater. **224**, 143 (2001).
[6] L. Wang, J. Ding, Y. Li, H. Z. Kong, Y. P. Feng, and X. Z. Wang, J. Phys.: Condens. Matter **12**, 4253 (2000).
[7] S. Yoshiike, H. Adachi, H. Ichinose, K. Tokumitsu, H. Ino, and K. Siratori, Mater. Trans., JIM **39**, 102 (1998).
[8] W. Zhang, A. Takeuchi and A. Inoue, Mater. Trans., JIM **38**, 1027 (1997).
[9] M. J. Kramer, A. S. O'Connor, K. W. Dennis, and R. W. McCallum (unpublished).
[10] R. Harris, M. Plischke, and M. J. Zuckermann, Phys. Rev. Lett. **31**, 160 (1973).
[11] M. C. Chi and R. Alben, J. Appl. Phys. **48**, 2987 (1977).
[12] E. Callen, Y. J. Liu, and J. R. Cullen, Phys. Rev. B **16**, 263 (1977).
[13] E. M. Chudnovsky, R. A. Serota, and W. M. Saslow, Phys. Rev. B **33**, 251 (1986).
[14] W. M. Saslow, Phys. Rev. B **35**, 3454 (1987).
[15] N. Hamamoto, N. Onishi, and G. Bertsch, Phys. Rev. B **61**, 1336 (2000).
[16] R. Skomski and D. J. Sellmyer, J. Appl. Phys. **87**, 4756 (2000).
[17] J. Arcas, A. Hernando, J. M. Barandiaran, C. Prados, M. Vazquez, P. Marin, and A. Neuweiler, Phys. Rev. B **58**, 5193 (1998); I. Navarro, M. Ortuno, and A. Hernando, *ibid.* **53**, 11 656 (1996); A. Hernando, P. Marin, M. Vazruez, J. M. Barandiaran, and G. Herzer, *ibid.* **58**, 366 (1998).
[18] R. Skomski, J. P. Liu, and D. J. Sellmyer, Phys. Rev. B **60**, 7359 (1999).
[19] M. El-Hilo, R. W. Chantrell, and K. O'Grady, J. Appl. Phys. **84**, 5114 (1998).
[20] P. Allia, M. Coisson, M. Knobel, P. Tiberto, and F. Vinai, Phys. Rev. B **60**, 12 207 (1999).
[21] T. Schrefl, J. Fidler, and H. Kronmuller, Phys. Rev. B **49**, 6100 (1994).
[22] P. A. Lindgard, P. V. Hendriksen, Phys. Rev. B **49**, 12 291 (1994).
[23] J. P. Bucher and L. A. Bloomfield, Phys. Rev. B **45**, 2537 (1992).
[24] P. V. Hendriksen, S. Linderoth, and P. A. Lindgard, Phys. Rev. B **48**, 7259 (1994).
[25] K. Binder and D. W. Heerman, *Monte Carlo Simulation in Satistical Physics*, Springer Series in Solid State Science, Vol. 80 (Springer, New York, 1988).
[26] M. E. J. Newman and G. T. Barkema, *Monte Carlo Methods in Statistical Physics* (Clarendon, Oxford, 1999).
[27] D. A. Dimitrov and G. M. Wysin, Phys. Rev. B **54**, 9237 (1996).
[28] J. Garcia-Otero, M. Porto, J. Rivas, and A. Bunde, J. Appl. Phys. **85**, 2287 (1999).
[29] Jesus Garcia-Otero, Markus Porto, Jose Rivas, and Armin Bunde,

Phys. Rev. Lett. **84**, 167 (2000).
[30] R. Smirnov-Rueda, O. Chubykulo, V. Nowak, R. W. Chantrell, and J. M. Gonzalea, J. Appl. Phys. **87**, 4798 (2000).
[31] U. Nowak, R. W. Chantrell, and E. C. Kennedy, Phys. Rev. Lett. **84**, 163 (2000).
[32] D. N. H. Nam, K. Jonason, P. Nordblad, N. V. Khiem, and N. X. Phuc, Phys. Rev. B **59**, 4189 (1999).
[33] J. Tejada, B. Martinez, A. Labarta, R. Grossinger, H. Sassik, M. Vazquez, and A. Hernando, Phys. Rev. B **42**, 898 (1990).
[34] R. W. Chantrell, N. S. Walmsley, J. Gore, and M. Maylin, J. Appl. Phys. **85**, 4340 (1999).
[35] X. G. Li, X. J. Fan, G. Ji, W. B. Wu, K. H. Wong, C. L. Choy, and H. C. Ku, J. Appl. Phys. **85**, 1663 (1999).
[36] C. P. Bean and J. D. Livingston, J. Appl. Phys. **30**, 120S (1959).
[37] J. Ding, P. G. McCormick, and R. Street, J. Magn. Magn. Mater. **124**, 1 (1993).
[38] S. Chikazumi, *Physics of Magnetism* (Krieger, Malabar, FL, 1964).
[39] K. Roll, in *Magnetic Multilayers and Giant Magnetoresistance*, edited by G. Ertl, R. Gomer, H. Luth, and D. L. Mills (Springer, New York, 1999), p. 13.